NEOPLASIA
www.neoplasia.com

Volume 21 Number 3 March 2019 pp. 257–268 257

Neuroblastoma RAS Viral Oncogene Homolog (NRAS) Is a Novel Prognostic Marker and Contributes to Sorafenib Resistance in Hepatocellular Carcinoma[1]

Peter Dietrich[*,†], Anne Gaza[*], Laura Wormser[*], Valerie Fritz[*], Claus Hellerbrand[*,‡] and Anja Katrin Bosserhoff[*,‡]

[*]Institute of Biochemistry, Emil-Fischer-Zentrum, Friedrich-Alexander-University Erlangen-Nürnberg, Erlangen, Germany; [†]Department of Medicine 1, University Hospital Erlangen, Friedrich-Alexander-University Erlangen-Nürnberg, Erlangen, Germany; [‡]Comprehensive Cancer Center (CCC) Erlangen-EMN, Erlangen, Germany

Abstract

Inhibition of the RAS-RAF-ERK-pathway using sorafenib as a first-line and regorafenib as a second-line treatment approach is the only effective therapeutic strategy for advanced hepatocellular carcinoma (HCC). Recent studies suggest that wild-type KRAS and HRAS isoforms could majorly contribute to HCC progression and sorafenib resistance. In contrast, the role of *neuroblastoma RAS viral oncogene homolog* (NRAS) in HCC remained elusive. In this study, wild-type NRAS was found to be overexpressed in HCC cell lines, preclinical HCC models, and human HCC tissues. Moreover, NRAS overexpression correlated with poor survival and proliferation *in vivo*. However, siRNA-pool–mediated NRAS knockdown showed only slight effects on HCC proliferation, clonogenicity, and AKT activity. We determined that KRAS upregulation served as a functional compensatory mechanism in the absence of NRAS, which was overcome by combined inhibition of NRAS and KRAS in HCC cells. Furthermore, NRAS expression was elevated in sorafenib-resistant compared to nonresistant HCC cells, and NRAS knockdown enhanced sorafenib efficacy in resistant cells. In summary, NRAS appears to be a prognostic marker in HCC and contributes to sorafenib resistance. Regarding potential therapeutic strategies, NRAS inhibition in HCC should be combined with KRAS inhibition to prevent KRAS-mediated rescue effects.

Neoplasia (2019) 21, 257–268

Introduction

Hepatocellular carcinoma (HCC) is a major cause of cancer-related mortality [1,2]. Sorafenib as a first-line [3–5] and regorafenib as a second-line [6] approach are the only effective therapeutic strategies for advanced HCC. Both sorafenib and regorafenib target multiple kinase-related pathways including the RAS-RAF-ERK-pathway in HCC cells, underlining the crucial role of RAS signaling in HCC [3,7,8]. In most recent studies, our group showed that the wild-type RAS isoform *Kirsten rat sarcoma* (KRAS) is a promising candidate diagnostic and therapeutic target majorly contributing to acquired resistance to RAF inhibitors in HCC and other types of cancer [9–11]. Moreover, we found that the *HRas proto-oncogene* (HRAS) isoform is upregulated in HCC and affects patient outcome [12].

Unlike KRAS and HRAS, the precise function of *neuroblastoma RAS viral oncogene homolog* (NRAS) was unclear in HCC. Mouse models of primary liver cancer driven by oncogenic NRAS have been established previously [13]; however, several studies suggested that NRAS mutations only rarely occur in human HCC [14,15]. In contrast to mutated NRAS, the role of wild-type NRAS in HCC progression and therapy resistance remained completely unknown and was addressed in this study.

Address all correspondence to Anja Katrin Bosserhoff, PhD, Institute of Biochemistry, Emil-Fischer-Zentrum, FAU Erlangen-Nürnberg, 91054 Erlangen, Germany.
E-mail: anja.bosserhoff@fau.de

[1] Conflict of Interest Statement: Conflict of Interest Statement.

Received 17 August 2018; Revised 28 October 2018; Accepted 27 November 2018

1476-5586
https://doi.org/10.1016/j.neo.2018.11.011

Materials and Methods

Cells and Cell Culture

The human HCC cell lines PLC (ATCC CRL-8024), HepG2 (ATCC HB-8065), and Hep3B (ATCC HB-8064) were described previously [11]. Murine Hepa129 cells originate from a C3H/HeN mouse and were obtained from the NCI-Frederick Cancer Research and Development Center (DCT Tumour Repository). Sorafenib-resistant HCC cells (Hep3B) were generated by long-term (3-4 months) exposure of cells to sorafenib with stepwise dose escalation (0.5 μM per week) up to 10 μM [11]. In parallel, nonresistant, untreated Hep3B cells were cultured and used as controls. As soon as the resistant cells were able to tolerate 8 μM of sorafenib without signs of toxicity, proliferation and anchorage-dependent growth assays were performed. Sorafenib ("Nexavar") was purchased from Selleckchem (Munich, Germany). Primary human hepatocytes were isolated as described [16].

Human Material

Paired human HCC tissues and corresponding nontumorous liver tissues originated from patients that underwent partial hepatectomy. The tissue microarray comprising paraffin-embedded human HCC tissue samples was analyzed as described [11,17,18]. All experimental procedures were performed according to the guidelines of the nonprofit state-controlled Human Tissue and Cell Research (HTCR) foundation with informed patients' consent [18]. Sampling and handling of patient material were performed in accordance with the ethical principles of the Declaration of Helsinki.

Immunohistochemistry

Immunohistological analysis was performed as previously described [11]. In brief, after deparaffinizing/dewaxing in xylene and rehydration in a graded series of isopropanol, antigen retrieval was achieved by microwave in Tris-EDTA buffer. After peroxidase block (Dako, Hamburg, Germany), the sections were incubated with anti–phospho-ERK antibody (1 in 100 dilution; Cell Signaling, Frankfurt am Main, Germany), anti–Ki-67/MIB-1 (1 in 50 dilution, Dako GmbH, Hamburg, Germany) (Abcam, Cambridge, UK; 1 in 2,000 dilution), anti-KRAS antibody (1 in 50 dilution; Abcam), or a validated and specific NRAS antibody (1 in 200 dilution, Abcam). As a next step, the slides were washed three times with PBS and then incubated with HRP-labeled polymer (conjugated with anti-rabbit secondary antibody) before again washing three times with PBS. Staining was performed with DAB (Dako) followed by counterstaining with hematoxylin (Merck, Darmstadt Germany). NRAS staining was described qualitatively using "0" ("low/negative"), "1" ("moderate"), or "2" ("high"). KRAS membrane localization was described qualitatively using "0" ("negative": cytoplasmic/endomembranous staining), "1" ("positive": <50% of cells show positive plasma membrane staining), or "2" ("strong positive": >50% of cells show positive plasma membrane staining). Quantification of pERK staining ("0": <5%; "1": 5%-20%; "2" more than 20% positive cells) was also performed in HCC tissues.

Protein Analysis

Protein extraction and Western blotting analysis were performed as described elsewhere [11]. The following antibodies were used: anti–phospho-ERK (1 in 4000 dilution; Cell Signaling, Frankfurt am Main, Germany), anti-ERK (1 in 1000 dilution; Cell Signaling), anti-KRAS antibody (1 in 1000 dilution; Abcam), anti–phospho-AKT (1 in 2000 dilution; Cell Signaling), anti-AKT (1 in 2000 dilution; Cell Signaling), and anti-NRAS (1 in 1000 dilution, Abcam). For visualization of immunoreactions, the NBT/BCIP (Sigma-Aldrich) staining technique was used. Computational densitometry of the scanned Western blot images was performed using the "ImageJ" program (National Institutes of Health, USA).

Cell Proliferation, Clonogenicity and Migration Analysis

The xCELLigence System (Roche) was used to analyze real-time cell proliferation as described previously [11]. Stem cell properties of cancer cells (clonogenicity) were analyzed using clonogenic assays as described [12]. Cell migration was analyzed using the Boyden chamber system as described [9].

RNA Expression Analysis

Total RNA isolation and reverse transcription were performed as described previously [11]. Quantitative reverse-transcription polymerase chain reaction (qRT-PCR) was performed using a Lightcycler (Roche, Mannheim, Germany) as described [9]. The following primer pairs were used: 18S (5′-GCA ATT ATT CCC CAT GAA CG-3′ and 5′-GGG ACT TAA TCA ACG CAA GC-3′), BAX (5′-TGC AGA GGA TGA TTG CCG CCG TGG-3′ and 5′-CAC CCA ACC ACC CTG GTC TTG GA TC-3′), BCL-2 (5′-AGG CAC CCA GGG TGA TGC AA-3′ and 5′-GTG GAG GAG CTC TTC AGG GA-3′), BCL-3 (5′- TGA CAG CAG CCT CAA GA AC-3′ and 5′-CGG AGA GAA GAC CAT TG GA-3′), HRAS (5′-TGG TGG GGA ACA AGT GTG AC-3′ and 5′-TTG TGC TGC GTC AGG AGA G-3′), KRAS (5′-TGG AGC TGG TGG CGT AGG CA-3′ and 5′-AGC CCT CCC CAG TCC TCA TGT-3′), LIN28 (5′-CGG TGC GGG CAT CTG TAA GT GG-3′ and 5′-TGG CCG CCT CTC ACT CCC AAT AC-3′), MAPK14 (5′-GGT AAA ATC TCG GCT CTC GG-3′ and 5′-CTC CGG CGC TCA AGA CTG-3′), and NRAS (5′-ATG AGG ACA GGC GAA GG CT-3′ and 5′-TGA GTC CCA TCA TCA CTG CTG-3′).

Quantification of Apoptosis

Fluorescence-activated cell sorting and the "ApoDETECT ANNEXIN V-FITC KIT" (Invitrogen distributed by Life Technologies, Darmstadt, Germany) were used to quantify apoptotic cells as described earlier [19].

Transfecting Cells with Si-RNA-Pools and MicroRNAs

A total of 2×10^4 cells were seeded per well in six-well plates. The Lipofectamine RNAimax transfection reagent was used (Life Technologies, Darmstadt, Germany). Si-RNA-pools against the human HRAS, KRAS, and NRAS mRNAs were used (functionally verified by siTOOLs Biotech GmbH, Planegg, Germany). Si-RNA-Pools consist of 30 single si-RNAs and are considered to reduce off-target effects [9]. For transfection of microRNAs, 5 μl (20 mM per microRNA) of commercially available pre-miR-622 (Ambion) and the corresponding pre-miR negative Control #1 (Ambion) were transfected per six-well plate. Total RNA and protein were isolated for 48 hours after transfection as described [9].

In Silico Analysis

In silico analysis of RNA expression of NRAS was performed using Gene Expression Omnibus (GEO) datasets (GEO profiles). A murine Mdr2-knockout HCC model-derived dataset was used. The Mdr2-KO mouse represents a model for a beta-catenin–negative subgroup of human HCCs characterized by downregulation of multiple tumor suppressor genes [20]. Additionally, the Trim24-KO murine HCC

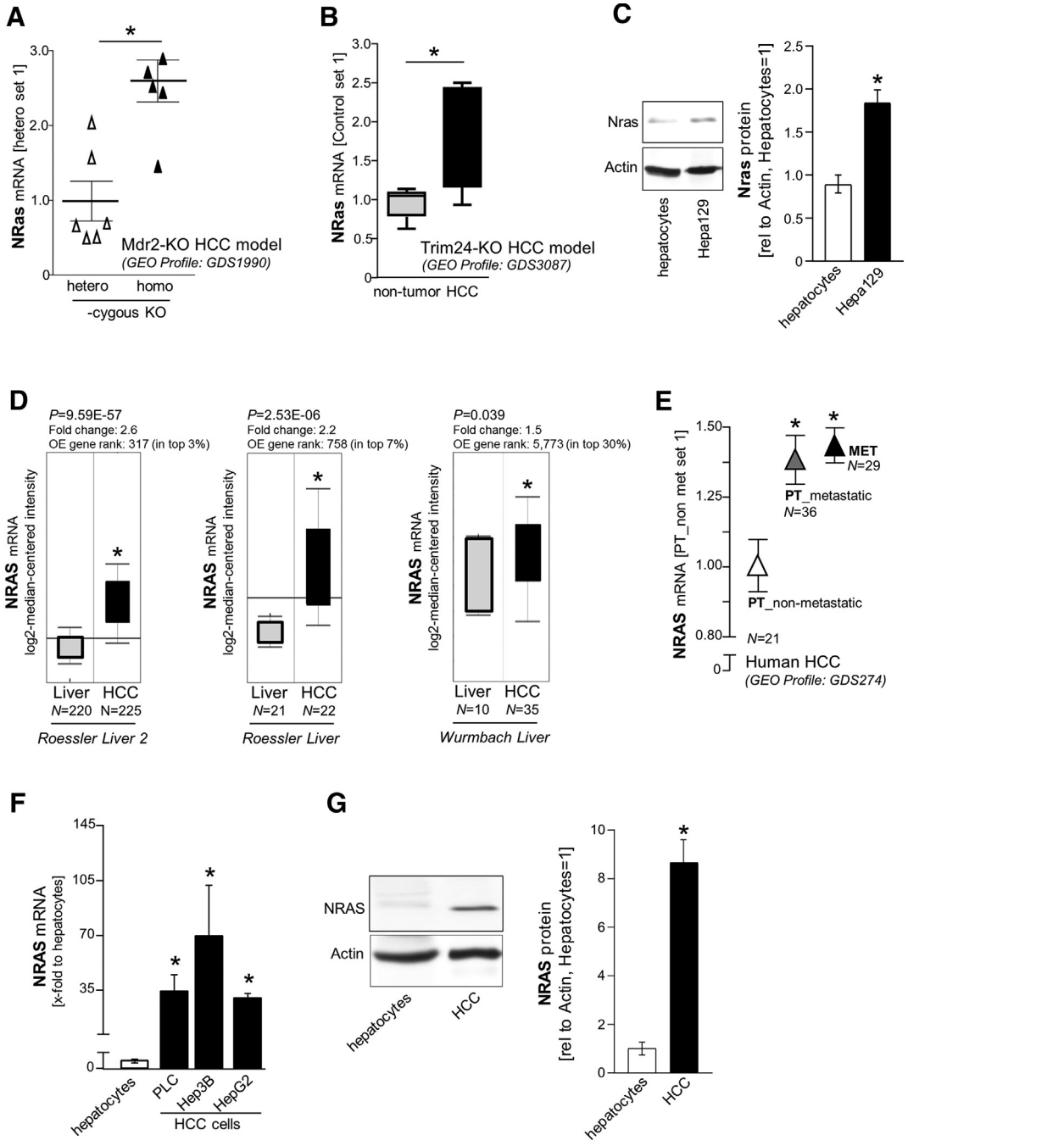

Figure 1. Expression of NRAS in HCC. (A) Nras mRNA levels in liver tissues derived from homo- ($N=6$) as compared to heterozygous ($N=6$) Mdr2-knockout (KO) mice (*: $P<.05$). (B) Nras mRNA levels in HCC ($N=6$) as compared to nontumor liver tissues ($N=6$) derived from a Trim24-knockout (KO) mouse model (*: $P<.05$). (C) Nras protein levels (Western blot analysis) in murine HCC cells (Hepa129) as compared to primary murine hepatocytes (*: $P<.05$ vs. hepatocytes). (D) NRAS mRNA levels in nontumorous liver tissues ("Liver") as compared to HCC patient tissues. Data were obtained from the Oncomine cancer microarray database using the datasets "Roessler Liver 2," "Roessler Liver," and "Wurmbach Liver" (OE: overexpression) (*: $P<.05$ vs. "Liver"). (E) GEO dataset analysis comparing NRAS expression in human metastatic HCC tissues ("MET") as well as primary tumor tissues that had metastasized ("PT_metastatic") and nonmetastatic HCC tissues ("nonmetastatic") (*: $P<.05$ vs. "nonmetastatic"). (F) NRAS mRNA expression levels (qRT-PCR analysis) in human HCC cell lines (PLC, Hep3B, HepG2) as compared to primary human hepatocytes (*: $P<.05$ vs. hepatocytes). (G) Summarized NRAS protein expression (Western blot analysis) in human HCC cell lines (PLC, Hep3B, HepG2) as compared to primary human hepatocytes (*: $P<.05$ vs. hepatocytes) The exemplary Western blot image shows NRAS expression in hepatocytes compared with the HepG2 HCC cell line.

model was used to determine gene expressions in wild-type as compared to Trim24-deficient mice. Trim24 knockout mice also spontaneously develop HCCs [21]. Immunostainings of NRAS in human tissues were explored using the human proteinatlas (https://www.proteinatlas.org/) database. Oncomine cancer microarray database analysis for gene expressions was performed using the website https://www.oncomine.org/. Kaplan-Meier survival curve analysis was performed using the SynTarget/BioProfiling database [22,23].

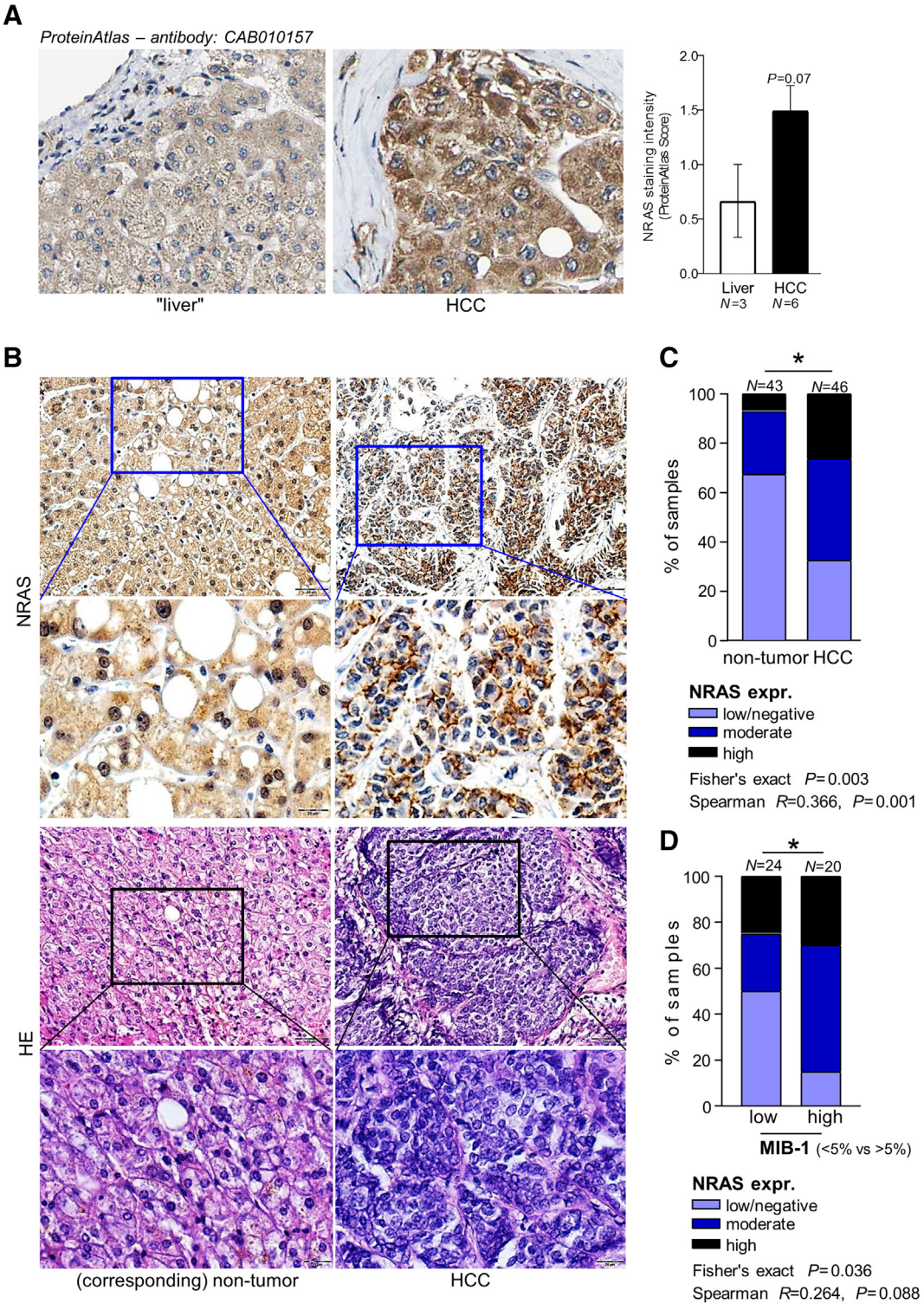

Figure 2. Immunohistochemical analysis of NRAS protein expression in human patient tissues. (A) NRAS staining (exemplary images and summarized staining intensity score) of nontumorous liver tissues ($N=3$) and HCC tissues ($N=6$) that were deposited on the human proteinatlas database. (B, C) Immunohistological analysis of NRAS protein expression in human HCC samples and corresponding nontumorous liver tissues applying a tissue microarray. Exemplary paired samples are depicted in B (NRAS and HE staining). A summarized quantification is depicted in C. (D) Tissue microarray analysis of NRAS expression levels in HCC tissues with low (<5% positive cells) or high (>5% positive cells) MIB-1 expression score (*: $P=.036$).

Additionally, the "SurvExpress-Biomarker validation for cancer gene expression" database (http://bioinformatica.mty.itesm.mx:8080/Biomatec/SurvivaX.jsp) was used as described [24].

Statistical Analysis

All results are expressed as mean ± SEM. The Student's t test or one-way analysis of variance, if appropriate, was used for statistical

Table 1. NRAS Immunoreactivity in HCC Tissues of 46 Patients in Relation to Clinicopathological Characteristics

Clinicopathological Characteristic	Categorization	*n* (%)	NRAS IR			*P**
			Low (Score 0)	Moderate (Score 1)	High (Score 2)	
Age at diagnosis	<60 years	24 (50.0)	6	10	8	.567
	≥60 years	22 (45.8)	9	8	5	
	ND	2 (4.2)	0	2	0	
Gender	Female	11 (23.9)	3	2	6	.072
	Male	33 (71.8)	12	15	6	
	ND	2 (4.3)	0	2	0	
Tumor stage	pT1	7 (16.3)	1	5	2	.334
	pT2	12 (27.9)	3	5	4	
	pT3	20 (46.4)	8	7	5	
	pT4	2 (4,7)	0	0	2	
	ND	2 (4.7)	0	2	0	
Histological grade	G1	14 (30.5)	4	9	1	.067
	G2	26 (56.5)	10	6	10	
	G3	4 (8.7)	1	2	1	
	ND	2 (4.3)	0	2	0	
Proliferation rate (MIB-1–pos. cells)	<5%	24 (52.2)	12	6	6	**.036**
	≥5%	20 (43.5)	3	11	6	
	ND	2 (4.3)	0	2	0	
KRAS activation (membrane staining)	<5%	22 (47.9)	11	9	2	**.047**
	≥5%	17 (37.0)	3	8	6	
	ND	7 (15.3)	1	2	4	

ND, no data available; *IR*, immunoreactivity.
* Fisher's exact test (two-sided); bold face representing *P* values <.05.

comparisons between groups. The level of significance was $P<.05$ ("ns": nonsignificant; "*": $P<.05$). The number of independent experiments was $n\geq 3$ (if not depicted otherwise). Calculations were performed using the GraphPad Prism Software (GraphPad Software, Inc., San Diego, CA) and SPSS (SPSS Statistics 23, IBM Corp., Armonk, NY).

Results

Expression of Wild-Type NRAS in HCC

First, we aimed at investigating the expression of NRAS in murine and human HCC models, cell lines, and patient tissues. The Mdr2-knockout (KO) mouse represents an established model of human HCC development [20]. GEO dataset analysis revealed that Nras was significantly overexpressed in homozygous as compared to heterozygous Mdr2-KO mice (Figure 1*A*), pointing to a potential role of Nras in HCC development in this model system. Trim24-deficient (KO) mice represent another experimental model of hepatocarcinogenesis [21]. A Trim24-KO mouse–derived GEO dataset showed significant elevation of Nras in established HCC tissues compared with control livers (Figure 1*B*). Likewise, Nras protein was markedly overexpressed in murine HCC cells as compared to primary murine hepatocytes (Figure 1*C*). In human HCC, *in silico* analysis using the Oncomine cancer microarray database [25] revealed significant upregulation of NRAS expression levels in HCC tissues compared with nontumorous livers in different patient-derived datasets [26,27] (Figure 1*D*). Regarding HCC progression, another GEO dataset revealed that NRAS was significantly upregulated in human metastatic HCC tissues and primary tumor tissues that had metastasized as compared to nonmetastatic HCCs (Figure 1*E*). Accordingly, both NRAS mRNA (Figure 1*F*) and protein (Figure 1*G*; Suppl. Figure 1) expression levels were strongly upregulated in human HCC cell lines (PLC, Hep3B, HepG2) as compared to primary human hepatocytes. Addressing a potential mechanism of upregulation of NRAS, we found that, in contrast to KRAS which was shown to be regulated by microRNA-622 by our group [11], NRAS revealed no binding sites for the KRAS-targeting microRNA-622 and was not regulated by this microRNA in HCC cells (Suppl. Figure 2), suggesting that different RAS isoforms have specific functional roles in cancer. In line with other studies that investigated tissue samples [14,15], Sanger sequencing revealed no oncogenic mutations in all three NRAS hotspots (codons 12, 13, and 61) [28] in human HCC cell lines (Hep3B, HepG2, PLC) (data not shown). Analysis of NRAS protein levels *in vivo* using the human proteinatlas database (www.proteinatlas.org) [29] pointed to overexpression of NRAS protein in HCC (only three "normal livers" and six HCC samples were available, but also in this small cohort, NRAS tended to be upregulated) (Figure 2*A*; Suppl. Figure 3*A*). To confirm these *in silico*–derived data in a larger patient cohort, immunohistochemistry analysis of tissue microarrays comprising human HCC tissues [11,17,18] was performed. Here, NRAS protein was significantly upregulated in HCC tissues compared with corresponding nontumorous liver tissues (Figure 2, *B* and *C*; Suppl. Figure 3*B*). Moreover, enhanced NRAS expression correlated with higher MIB-1 proliferation score in HCC patient tissues (Figure 2*D*; Table 1). Together, expression of wild-type NRAS was strongly enhanced in HCC cell lines and tissues, and increased NRAS expression levels correlated with liver cancer development, metastatic progression, and proliferation.

Effect of NRAS Expression on HCC Patient Survival

The strong overexpression of NRAS prompted us to ask whether NRAS expression could affect survival of HCC patients. Kaplan-Meier (overall) survival analysis was performed using the "SynTarget/BioProfiling" database and a The Cancer Genome Atlas (TCGA) HCC dataset [22,23]. High NRAS expression was a predictor for poor patient outcome (i.e., overall survival) ($N=370$, $P=.0211$) (Figure 3*A*). Poorer outcome of patients with high as compared to low NRAS expression by both "best separation" ($P<.0001$) and "median separation" ($P=.0045$) was confirmed using additional TCGA data

available from the human proteinatlas database (Suppl. Figure 4). Moreover, survival analysis using the "SurvExpress" Biomarker validation for cancer gene expression database [24] was performed. Computational stratification into "low-risk" and "high-risk" patient groups (based on prognostic index) revealed marked overexpression of NRAS as well as reduced overall survival of high- compared to low-risk groups in three available datasets (Figure 3*B*). In summary, these results indicated high NRAS expression as a predictor of poor outcome in HCC patients.

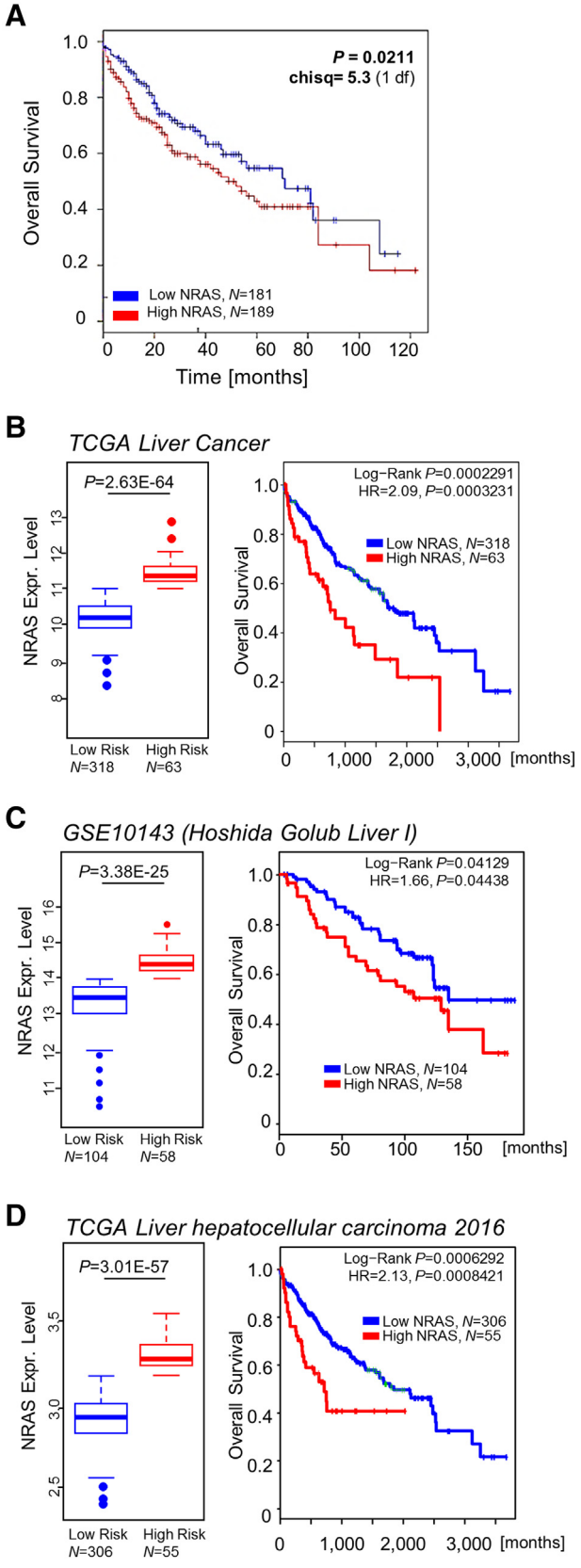

Function of Wild-Type NRAS in HCC

To further explore the role of NRAS in HCC, we performed functional analysis after NRAS suppression in HCC cells *in vitro*. A si-RNA-pool ("si-NRAS": functionally verified pool of 30 single si-RNAs against the human NRAS mRNA) and an corresponding si-RNA-control-pool ("Control") were used for specific gene knockdown and concomitant reduction of off-target effects. NRAS knockdown was established in two HCC cell lines (Hep3B, PLC) (Figure 4, *A* and *B*). Si-NRAS–treated HCC cells showed slight, nonsignificant reduction of proliferation (Figure 4*C*). Moreover, NRAS knockdown significantly reduced clonogenicity in Hep3B cells (Figure 4*D*). However, only slight, nonsignificant inhibition of colony formation was observed in PLC cells (P=.07) (Figure 3*D*). HCC cell migration was also not affected by NRAS knockdown as determined using Boyden chamber assays (Figure 3*E*). Western blot analysis revealed that, only in Hep3B cells, NRAS knockdown was sufficient to significantly impair AKT activation (Figure 3*F*). AKT activity was not affected in PLC cells, and ERK activity was not altered in both HCC cell lines after NRAS knockdown (Figure 3, *F* and *G*). In summary, NRAS suppression did not affect migration and ERK activation and had only moderate and partially nonsignificant effects on proliferation, clonogenicity, and AKT activation in HCC.

Loss of NRAS in HCC Cells Is Rescued by KRAS Upregulation

In the light of the strong overexpression of NRAS (Figure 1 and 2) and the marked effects on HCC patient survival (Figure 3), we had expected stronger functional effects (Figure 4) after NRAS knockdown or in all HCC cell lines, respectively. Interestingly, NRAS immunoreactivity was found to be significantly correlated with KRAS membrane staining in patient-derived tissue microarray samples (Table 1). Moreover, in contrast to NRAS expression "alone" [which did not correlate with ERK activation in patient-derived HCC tissues (N=45, Fisher's exact P=.134, Spearman R=0.194, P=.214)], co-positivity for both NRAS and KRAS staining was significantly correlated with ERK-activation (N=37, Fisher's exact P=.042, Spearman R=0.374, P=.042). Therefore, we hypothesized that NRAS might co-function with other RAS isoforms and that loss of NRAS in HCC cells could potentially be compensated by other RAS proteins. To adress this hypothesis, the canonical "non-NRAS" RAS isoforms (i.e., KRAS and HRAS) were knocked down in HCC cells (Hep3B, PLC) using si-RNA-pool–mediated mRNA suppression. Here, combined si-HRAS and si-KRAS treatment served as "control"

Figure 3. Effect of NRAS expression on HCC patient survival. (A) Kaplan-Meier survival curve analysis was performed using the *SynTarget/BioProfiling* database for a TCGA HCC (LIHC) dataset (377 patient samples in total). Survival curves are depicted for the total patient cohort: "all patients" ["chisq": chi square; "df": degree(s) of freedom]. (B-D) "SurvExpress-Biomarker validation for cancer gene expression" database analysis of NRAS expression (*left panels*) and corresponding Kaplan-Meier curves for overall survival (*right panels*) in different datasets ["TCGA Liver Cancer" (B), "GSE10143" (C), and "TCGA Liver hepatocellular carcinoma June 2016" (D)]. Computational stratification into "low-risk" and "high-risk" patient groups was based on prognostic index (*HR*: hazard ratio).

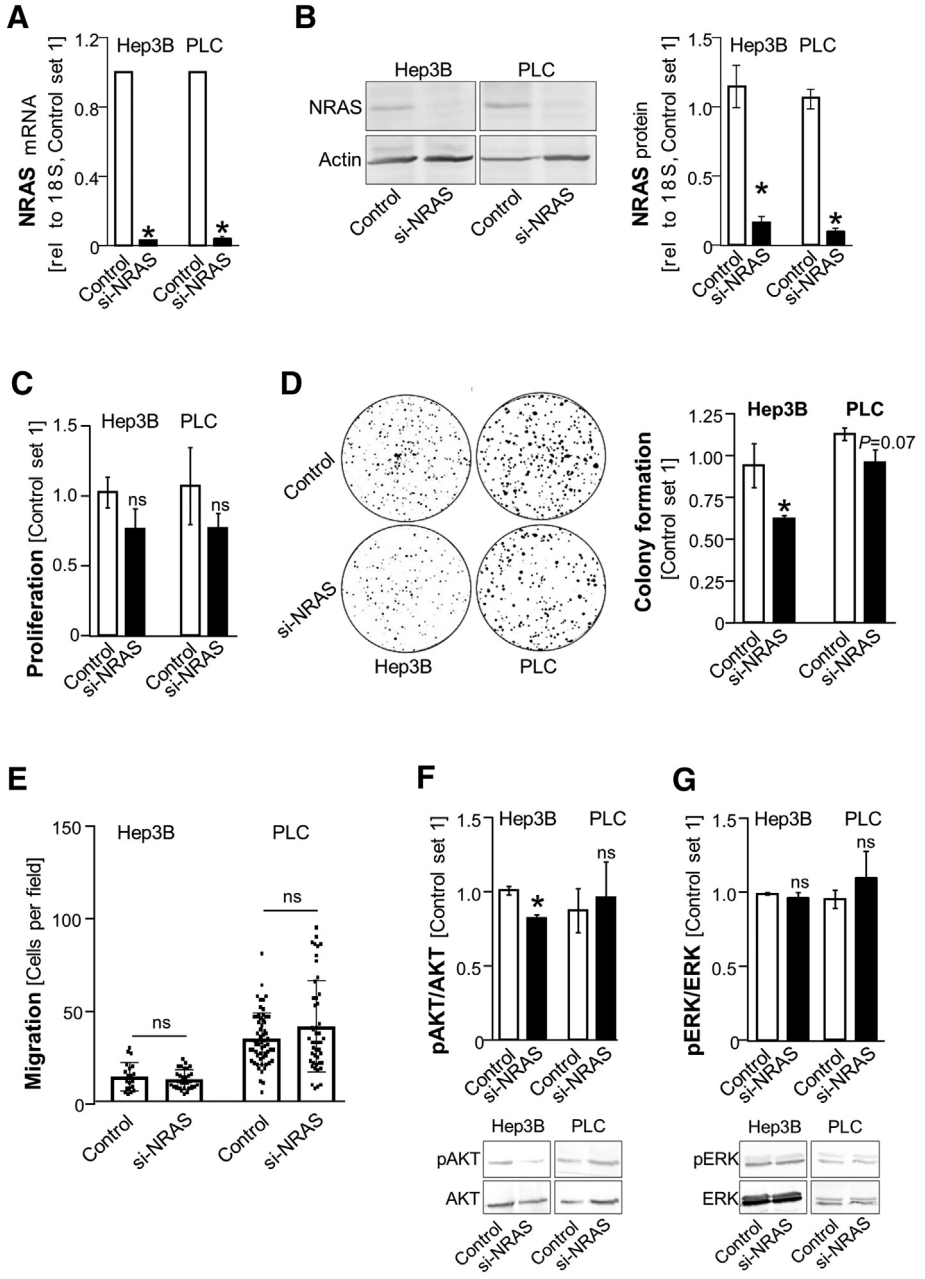

Figure 4. Function of wild-type NRAS in HCC. HCC cell lines (Hep3B, PLC) were transfected (48 hours) using a control-si-RNA-pool (Control) or a si-RNA-pool against the NRAS mRNA (si-NRAS). (A-B) NRAS mRNA (A) and protein levels (B) as well as corresponding exemplary Western blot images (B) (*: $P<.05$ vs. Control). (B) Real-time cell proliferation analysis (xCELLigence) (ns: nonsignificant vs. Control). (C) Anchorage-dependent clonogenicity assays [*left side*: representative images, *right side*: quantification of colony numbers ("colony formation")] (*: $P<.05$ vs. Control). (D) Boyden chamber cell migration analysis (ns: nonsignificant). (E, F) AKT (D) and ERK (E) activation (phospho-AKT/ERK in relation to AKT/ERK) as quantified by densitometric Western blot analysis and corresponding exemplary Western blot images (*: $P<.05$ vs. Control; ns: nonsignificant vs. Control).

and was compared to cells that were additionally treated with si-NRAS. In the absence of KRAS and HRAS, knockdown of NRAS significantly impaired proliferation in both HCC cell lines (Figure 5*A*, Suppl. Figure 5). qRT-PCR analysis revealed that, after NRAS knockdown, KRAS was significantly upregulated (by ~20%) in HCC cells, while HRAS expression was unaffected (Figure 5*B*). We have previously demonstrated that KRAS inhibition strongly impairs proliferation in HCC [11]. Therefore, the current observations together with our previous study pointed to KRAS (and not HRAS) as a major functional rescue gene in the absence of NRAS. Accordingly, knockdown of HRAS alone did not affect proliferation in both HCC cell lines (Figure 5*C*). To confirm the hypothesis that specifically KRAS (and not HRAS) is sufficient to rescue NRAS knockdown in HCC, we performed additional proliferation analysis. Here, si-NRAS effects were analyzed in 1) the absence of HRAS (si-HRAS *versus* si-HRAS+si-NRAS) and 2) the absence of KRAS (si-KRAS *versus* si-KRAS+si-NRAS). In the absence of HRAS [which had shown no effect on proliferation (Figure 5*C*)], additional NRAS knockdown did not significantly reduce the proliferation capacity of HCC cells (Figure 5*D*). In contrast and in line with our previous

study [11], KRAS inhibition alone was sufficient to strongly reduce proliferation. Noteably, NRAS knockdown further enhanced inhibition of proliferation in the absence of KRAS (Figure 5*D*). In contrast, migration was not affected by combined NRAS and KRAS knockdown (Suppl. Figure 6). This resembled our previous study showing that KRAS alone also did not regulate migration [11] as well

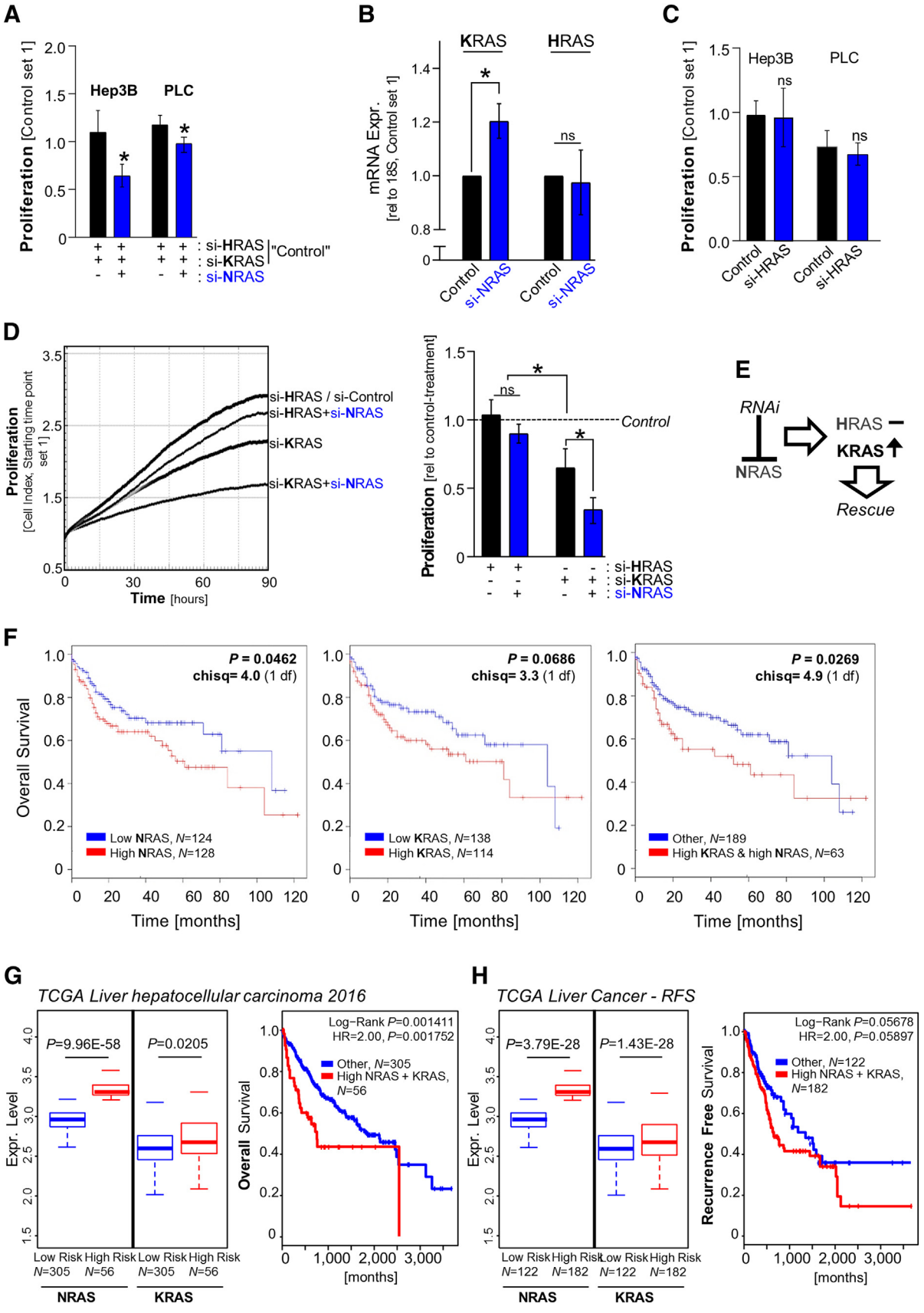

as the nonsignificant effects of single NRAS knockdown on migration seen in this study (Figure 4). Together, these data indicated that KRAS (but not HRAS) upregulation serves as a functional compensatory mechanism for HCC proliferation after loss of NRAS in HCC (Figure 5*E*). Based on our finding that NRAS affected survival in HCC (Figure 3; Suppl. Figure 4), we explored whether NRAS and KRAS might also co-function on patient survival. "SynTarget/BioProfiling" database analysis revealed a patient dataset with pronounced and significant effects on poor patient outcome of co-upregulated NRAS and KRAS levels (P=.0269, χ^2=4.9) compared to less/nonsignificant effects of upregulated "NRAS-only" (P=.0462, χ^2=4.0) or "KRAS-only" (P=.0686, χ^2=3.3) (Figure 5*F*). Moreover, "SurvExpress" Biomarker validation for cancer gene expression database analysis revealed significant co-upregulation of NRAS and KRAS and poorer overall (Figure 5*G*) and recurrence-free (Figure 5*H*) survival in high-risk as compared with low-risk patient groups. In summary, NRAS co-functioned with KRAS in HCC, and loss of NRAS was functionally rescued by KRAS upregulation.

Expression and Function of NRAS in Aquired Sorafenib Resistance

Since our previous study had revealed strong impact of wild-type KRAS on RAF inhibitor resistance in HCC [11], we next asked if also NRAS might affect sorafenib resistance. First, long-time exposure to slowly increasing doses of sorafenib was performed to establish sorafenib-resistant Hep3B and PLC cell clones. Functionally, these cells revealed marked resistance to sorafenib exposure compared to nonresistant cells (Figure 6, *A* and *B*). Moreover, the resistant cells showed enhanced epression of the chemoresistance-associated stem cell marker *Lin-28 homolog A* (LIN28A) [30] and sorafenib-resistance–induced *mitogen-activated protein kinase 14* (MAPK14) [31] (Figure 6*C*). NRAS but not HRAS mRNA expression was significantly upregulated in sorafenib-resistant as compared to nonresistant HCC cells (Figure 6*D*). Western blot analysis confirmed that also NRAS protein leveles were upregulated in sorafenib-resistant Hep3B cell clones as compared to nonresistant Hep3B cells (Figure 6*E*). Since resistant cells were cultured in sorafenib-containing medium to ensure constant selection pressure, we excluded that sorafenib treatment could directly induce NRAS expression in HCC cells (Suppl. Figure 7). Functionally, real-time cell proliferation analysis showed that si-RNA–mediated NRAS knockdown (alone) was sufficient to inhibit cell proliferation in sora-resistant HCC cells (Figure 6*F*). Resembling nonresistant cells, NRAS knockdown partially but however nonsignificantly upregulated KRAS but not HRAS in resistant cells (Suppl. Figure 8). Furthermore, NRAS knockdown did not affect apoptosis in these cells (Suppl. Figure 9) but restored sorafenib sensitivity in resistant cells (Figure 6*G*). In summary, these data revealed that in aquired resistance to sorafenib, HCC cells upregulate NRAS expression and NRAS inhibition could be sufficient to enhance sorafenib sensitivity. Regarding these data together with the previously described function of KRAS in sorafenib resistance [11], our findings suggest that co-targeting of NRAS and KRAS might be an effective therapeutic approach to overcome sorafenib resistance in HCC.

Discussion

Although RAS proteins are among the most desirable therapeutic targets in cancer, they were considered to be "undruggable" for a many years [4]. Meanwhile, technical improvements have resurrected the concept of effective RAS inhibition and promoted the so-called "RAS renaissance" [4,32–35]. In HCC, RAS proteins have commonly no mutations in the known hotspot regions [2,36]. NRAS and KRAS are mutated in <5% of HCCs [14]. Therefore, until recently, RAS proteins were only poorly investigated in HCC, and their potential diagnostic and therapeutic functions remained unclear.

Novel studies by our group demonstrated that wild-type KRAS can function as a potent therapeutic target in "non–KRAS-mutated" cancer types including malignant melanoma [9,10] and HCC [11]. At a first glance, melanoma and HCC are cancer types without remarkable similarities. However, apart from their primary sites, on a molecular level, both melanoma and HCC strongly depend on the RAS-RAF-ERK-pathway. In advanced melanoma, specific BRAF inhibition represented the only effective therapeutic option for many years and is still considered as a first-line therapeutic strategy for patients with $BRAF^{V600E}$ mutations [37]. Likewise, the unspecific RAF inhibitors sorafenib and regorafenib are the only approved systemic therapy options for intermediate and advanced HCC patients [3,7,8]. We found recently that inhibition of wild-type KRAS inhibits proliferation, clonogenicity and RAS downstream signaling in melanoma and in HCC *in vitro* and *in vivo*. Moreover, both cancer types showed strong upregulation of wild-type KRAS, which was released by the downregulated tumor-suppressive microRNA-622 [10,11]. KRAS expression also correlated with tumor stages and patient survival [9,11]. Furthermore, we found that HRAS is a prognostic marker in HCC and revealed that the novel RAS inhibitor rigosertib exerted strong functional effects on HCC cells [12]. In summary, these previous studies highlighted the importance of wild-type RAS proteins in HCC.

In contrast to KRAS and HRAS, the role of NRAS in HCC was elusive. A recent transcriptome profiling study revealed that NRAS was dysregulated in fibrolamellar HCC, but potential clinical implications

Figure 5. Effects of NRAS knockdown on KRAS and HRAS expression and functional effects of combined NRAS and KRAS inhibition. HCC cell lines (Hep3B, PLC) were transfected (48 hours) using si-RNA-pools against the HRAS (si-HRAS), KRAS (si-KRAS), or the NRAS (si-NRAS) mRNA. (A) Real-time cell proliferation analysis (xCELLigence) (*: P<.05 vs. Control). (B) KRAS and HRAS mRNA expression levels (qRT-PCR analysis) in human HCC cell lines (the graph summarizes data for both PLC and Hep3B cells) (*: P<.05 vs. Control; ns: nonsignificant vs. Control). (C) Real-time cell proliferation analysis (xCELLigence) after knockdown of si-HRAS compared with control-transfected cells (ns: nonsignificant). (D) Real-time cell proliferation analysis (xCELLigence). The left panel depicts a representative image of proliferation curves, while the right panel depicts summarized quantifications (*: P<.05; ns: nonsignificant). (E) Hypothesis on KRAS-mediated functional rescue after RNAi-induced NRAS knockdown. (F) Kaplan-Meier survival curve analysis was performed using the *SynTarget/BioProfiling* database for a TCGA HCC (LIHC) dataset (377 patient samples in total). Survival curves are depicted for the patient cohort "N0-stage" ["chisq": chi square; "df": degree(s) of freedom]. (G,H) "SurvExpress" Biomarker validation for cancer gene expression database analysis of combined NRAS and KRAS expression (*left panels*) and corresponding Kaplan-Meier curves for overall (G) and recurrence-free (H) survival (*right panels*) in different datasets ["TCGA Liver hepatocellular carcinoma June 2016" (G) and "TCGA Liver Cancer" (H)]. Computational stratification into "low-risk" and "high-risk" patient groups was based on prognostic index (*HR*: hazard ratio).

or the function of NRAS have not been investigated [38]. Another recent study found that NRAS and c-MYC are co-upregulated by insulin-like growth factor II in HCC, but the specific function of NRAS was not explored [39]. Therefore, until now, there was no mechanistic evidence for the potential function of wild-type NRAS in HCC. Here, we newly demonstrated marked overexpression of wild-type NRAS in HCC cell lines, murine HCC models, and patient tissues, and NRAS expression correlated with poor patient survival. *In vitro* analysis using specific si-RNA-pool–mediated NRAS knockdown showed only slight effects on HCC cell proliferation, clonogenicity, and AKT activity, and

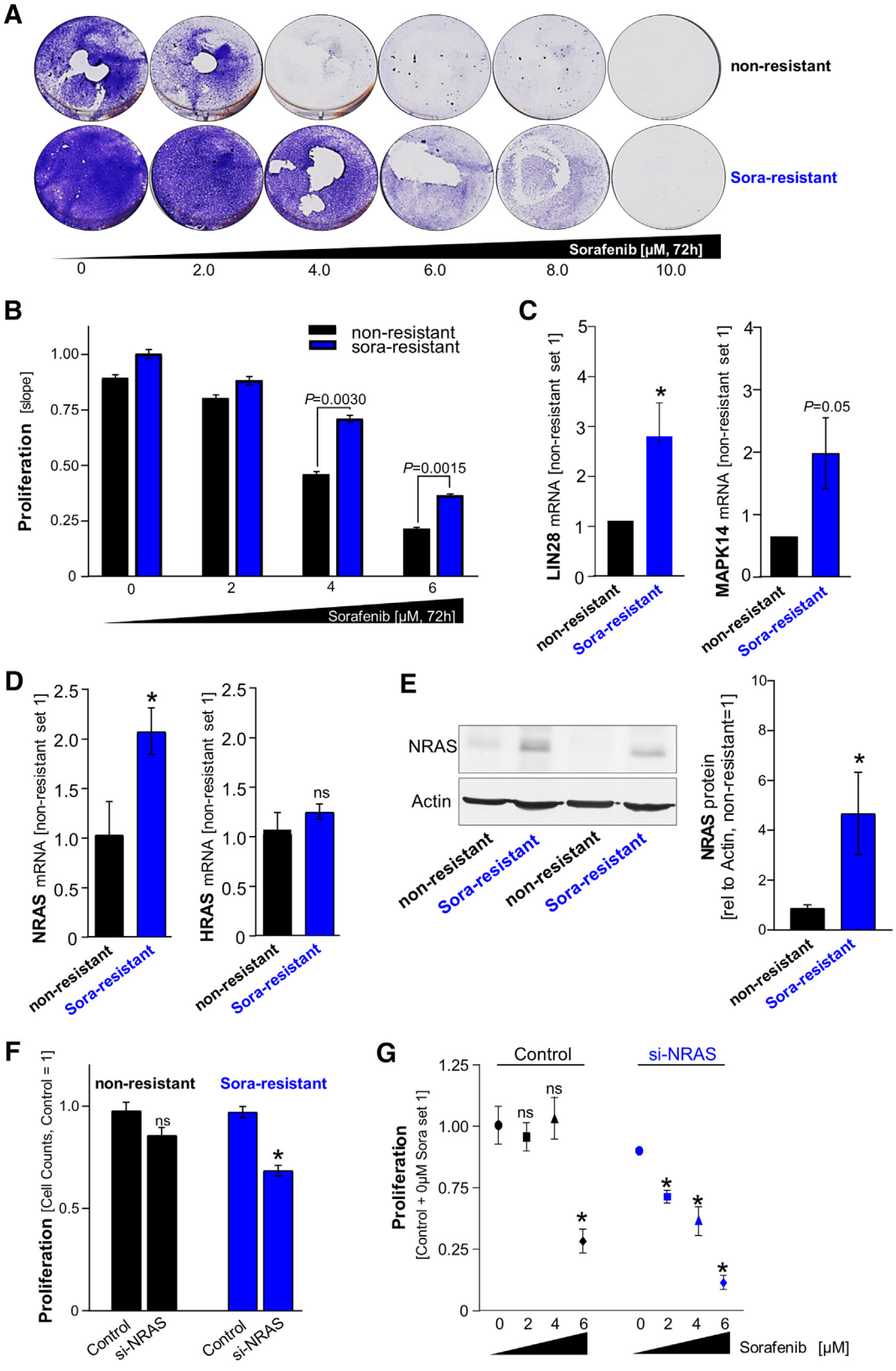

nonsignificant effects on migration and ERK activation. Significant reduction of clonogenicity and AKT-signaling after NRAS knockdown was found only in the Hepa3B cell line which had revealed the highest levels of NRAS mRNA as compared with other HCC cell lines used in this study. Strikingly, RAS-isoform–specific antibodies revealed that NRAS immunoreactivity correlated with KRAS membrane staining in patient-derived tissue samples. Further, in contrast to NRAS expression alone, co-positivity for both NRAS and KRAS staining significantly correlated with ERK activation. After NRAS knockdown, KRAS but not HRAS was upregulated in HCC cells, thereby rescuing pro-proliferation effects of NRAS. These data suppose that, apart from inhibition of KRAS [11], a combinatory approach targeting both KRAS and NRAS could be even more effective in HCC. HRAS, however, was indeed shown to serve as a prognostic marker in HCC [12] but did not affect proliferation or was sufficient to compensate for loss of NRAS in this study. These results are in accordance with novel findings that confirm specific functions of different RAS isoforms in other cancer types like pancreatic cancer [40]. Accordingly, in contrast to KRAS, NRAS revealed no binding sites for the KRAS-targeting microRNA-622 and was not regulated by this microRNA in HCC cells. Together, different RAS isoforms display nonexchangeable, specific functions in HCC and potentially also in other types of cancer.

The efficacy of RAS inhibition underlines the importance of RAS downstream signaling pathways such as the MAPK and the PI3K pathway. Moreover, it highlights the major clinical issue of acquired resistance to RAF inhibitors. Escape pathway activation of RAS-RAF-ERK is considered to be a crucial mediator of chemoresistance in HCC [5,41]. In our previous studies, wild-type KRAS was upregulated in (B)RAF-inhibitor–resistant cancer cells, and inhibition of KRAS could almost completely break resistance to vemurafenib [9] and sorafenib [11]. Also, other studies suggested wild-type KRAS as an emerging therapeutic target in cancer therapy resistance [42,43]. Accordingly, novel phase II/III clinical studies reveal that upstream inhibition of MAPK and PI3K pathways by, e.g., EGFR inhibition is sufficient in wild-type KRAS/NRAS colorectal cancer [44]. Another study highlighted the importance of wild-type RAS proteins by revealing that wild-type HRAS and NRAS promote mutant KRAS-driven tumorigenesis [45]. In the current study, NRAS expression was significantly overexpressed in sorafenib-resistant HCC cells compared to nonresistant cells. Moreover, NRAS knockdown partly restored sorafenib efficacy in resistant HCC cells. In contrast to nonresistant cells, NRAS inhibition alone was sufficient to significantly impair proliferation in resistant cells, and NRAS knockdown only slightly and nonsignificantly induced KRAS upregulation. These findings suggest that sorafenib-resistant cells more strongly depend on NRAS as compared to nonresistant cells.

In summary, this study indicates wild-type NRAS as a prognostic marker in HCC. Furthermore, combined NRAS and KRAS inhibition might represent a novel therapeutic approach which could be achieved by pharmacologic "pan-RAS" or "dual-RAS" (i.e., KRAS and NRAS) inhibition.

Acknowledgements

This work was supported by grants from the German Research Association (DFG) to A. B. (RTG 1962/1, BO1573, and FOR 2127), C. H. (FOR 2127 and KFO 262), and P. D. (RTG 1962/1); the German Cancer Aid (Deutsche Krebshilfe, to A.B.); the Bavarian Research Network for Molecular Biosystems (BioSysNet, to A.B.); the Else-Kröner-Fresenius Stiftung (EKFS, to P.D.); and the Interdisciplinary Center for Clinical Research (IZKF) Erlangen (J55, to P.D.; D24, to A.B.; ELAN 17/4, to C.H.). We thank Annette Serwotka, Darleen Schönwälder, and Rudolph Jung for excellent technical assistance. We acknowledge the HTCR Foundation for making human tissue available for research and Hepacult GmbH (Regensburg, Germany) for providing primary human hepatocytes for *in vitro* studies. We appreciate the complex data and sample analysis of the Biobank o.b. HTCR of the Ludwig-Maximilians-University Munich to provide the selected liver tissue samples.

Author Contributions

P. D., A. K. B., and C. H. conceived the project, analyzed the data, and wrote the manuscript. P. D., A. G., L. W., and V. F. designed the experiments.

Appendix A. Supplementary data

Supplementary data to this article can be found online at https://doi.org/10.1016/j.neo.2018.11.011.

References

[1] Dietrich P and Hellerbrand C (2014). Non-alcoholic fatty liver disease, obesity and the metabolic syndrome. *Best Pract Res Clin Gastroenterol* **28**(4), 637–653.
[2] Aravalli RN, Steer CJ, and Cressman EN (2008). Molecular mechanisms of hepatocellular carcinoma. *Hepatology* **48**(6), 2047–2063.
[3] Pascual S, Herrera I, and Irurzun J (2016). New advances in hepatocellular carcinoma. *World J Hepatol* **8**(9), 421–438.
[4] Ostrem JM and Shokat KM (2016). Direct small-molecule inhibitors of KRAS: from structural insights to mechanism-based design. *Nat Rev Drug Discov* **15**(11), 771–785.

Figure 6. Expression and function of NRAS in aquired sorafenib resistance. (A) Representative images of crystal violet–stained nonresistant and sorafenib-resistant ("Sora-resistant") Hep3B cells. A total of 100,000 cells were seeded in 6-well plates and allowed to attach for 6 hours. Subsequently, cells were treated with different doses of sorafenib (0, 2, 4, 6, 8, 10 μM) for 72 hours. (B) Real-time cell proliferation analysis (xCELLigence) of sorafenib-resistant and nonresistant HCC cells treated with different doses of sorafenib (0, 2, 4, 6 μM) for 128 hours (ns: nonsignificant vs. Control). (C) LIN28 and MAPK14 mRNA expression levels (qRT-PCR analysis) in nonresistant as compared to sorafenib-resistant ("Sora-resistant") Hep3B cells (*: P<.05 vs. nonresistant). (D) NRAS (left panel) and HRAS (right panel) mRNA expression levels (qRT-PCR analysis) in nonresistant as compared to sorafenib-resistant ("Sora-resistant") Hep3B cells (*: P<.05 vs. non-resistant). (E) Exemplary images (left panel) and densitometry (right panel, representing N=3 pairs) of Western blot analysis of NRAS protein levels in nonresistant compared to sorafenib-resistant ("Sora-resistant") Hep3B cells (*: P<.05 vs. nonresistant). (F) Proliferation (relative cell number after 72 hours of cultivation under normal conditions in serum-containing media) of si-NRAS as compared to control-transfected sorafenib-resistant and nonresistant HCC cells, respectively. (G) Real-time cell proliferation analysis (xCELLigence). Sora-resistant Hep3B cells were transfected with a control-si-RNA-pool (Control) or a si-RNA-pool against the NRAS mRNA (si-NRAS). After seeding, cells were allowed to attach for 24 hours. Afterwards, cells were treated with different doses of sorafenib (0, 2, 4, 6 μM) for 96 hours. The graph depicts summarized quantifications [*: P<.05 vs. untreated cells (i.e., 0 μM sorafenib)].

[5] Nishida N, Kitano M, Sakurai T, and Kudo M (2015). Molecular mechanism and prediction of sorafenib chemoresistance in human hepatocellular carcinoma. *Dig Dis* **33**(6), 771–779.

[6] Bruix J, Qin S, Merle P, Granito A, Huang YH, Bodoky G, Pracht M, Yokosuka O, Rosmorduc O, and Breder V, et al (2017). Regorafenib for patients with hepatocellular carcinoma who progressed on sorafenib treatment (RESORCE): a randomised, double-blind, placebo-controlled, phase 3 trial. *Lancet* **389**(10064), 56–66.

[7] Wilhelm SM, Carter C, Tang L, Wilkie D, McNabola A, Rong H, Chen C, Zhang X, Vincent P, and McHugh M, et al (2004). BAY 43-9006 exhibits broad spectrum oral antitumor activity and targets the RAF/MEK/ERK pathway and receptor tyrosine kinases involved in tumor progression and angiogenesis. *Cancer Res* **64**(19), 7099–7109.

[8] Llovet JM, Ricci S, Mazzaferro V, Hilgard P, Gane E, Blanc JF, de Oliveira AC, Santoro A, Raoul JL, and Forner A, et al (2008). Sorafenib in advanced hepatocellular carcinoma. *N Engl J Med* **359**(4), 378–390.

[9] Dietrich P, Kuphal S, Spruss T, Hellerbrand C, and Bosserhoff AK (2018). Wild-type KRAS is a novel therapeutic target for melanoma contributing to primary and acquired resistance to BRAF inhibition. *Oncogene* **37**(7), 897–911.

[10] Dietrich P, Kuphal S, Spruss T, Hellerbrand C, and Bosserhoff AK (2018 Sep). MicroRNA-622 is a novel mediator of tumorigenicity in melanoma by targeting Kirsten rat sarcoma. *Pigment Cell Melanoma Res* **31**(5), 614–629.

[11] Dietrich P, Koch A, Fritz V, Hartmann A, Bosserhoff AK, and Hellerbrand C (2018). Wild type Kirsten rat sarcoma is a novel microRNA-622-regulated therapeutic target for hepatocellular carcinoma and contributes to sorafenib resistance. *Gut* **67**(7), 1328–1341.

[12] Dietrich P, Freese K, Mahli A, Thasler WE, Hellerbrand C, and Bosserhoff AK (2018). Combined effects of PLK1 and RAS in hepatocellular carcinoma reveal rigosertib as promising novel therapeutic "dual-hit" option. *Oncotarget* **9**(3), 3605–3618.

[13] Huntzicker EG, Hotzel K, Choy L, Che L, Ross J, Pau G, Sharma N, Siebel CW, Chen X, and French DM (2015). Differential effects of targeting Notch receptors in a mouse model of liver cancer. *Hepatology* **61**(3), 942–952.

[14] Ding X, Yang Y, Han B, Du C, Xu N, Huang H, Cai T, Zhang A, Han ZG, and Zhou W, et al (2014). Transcriptomic characterization of hepatocellular carcinoma with CTNNB1 mutation. *PLoS One* **9**(5), e95307.

[15] Janku F, Kaseb AO, Tsimberidou AM, Wolff RA, and Kurzrock R (2014). Identification of novel therapeutic targets in the PI3K/AKT/mTOR pathway in hepatocellular carcinoma using targeted next generation sequencing. *Oncotarget* **5**(10), 3012–3022.

[16] Lee SM, Schelcher C, Demmel M, Hauner M, and Thasler WE (2013). Isolation of human hepatocytes by a two-step collagenase perfusion procedure. *J Vis Exp* (79).

[17] Bauer R, Valletta D, Bauer K, Thasler WE, Hartmann A, Muller M, Reichert TE, and Hellerbrand C (2014). Downregulation of P-cadherin expression in hepatocellular carcinoma induces tumorigenicity. *Int J Clin Exp Pathol* **7**(9), 6125–6132.

[18] Thasler WE, Weiss TS, Schillhorn K, Stoll PT, Irrgang B, and Jauch KW (2003). Charitable state-controlled foundation human tissue and cell research: ethic and legal aspects in the supply of surgically removed human tissue for research in the academic and commercial sector in Germany. *Cell Tissue Bank* **4**(1), 49–56.

[19] Wobser H, Dorn C, Weiss TS, Amann T, Bollheimer C, Buttner R, Scholmerich J, and Hellerbrand C (2009). Lipid accumulation in hepatocytes induces fibrogenic activation of hepatic stellate cells. *Cell Res* **19**(8), 996–1005.

[20] Katzenellenbogen M, Mizrahi L, Pappo O, Klopstock N, Olam D, Jacob-Hirsch J, Amariglio N, Rechavi G, Domany E, and Galun E, et al (2007). Molecular mechanisms of liver carcinogenesis in the mdr2-knockout mice. *Mol Cancer Res* **5**(11), 1159–1170.

[21] Jiang S, Minter LC, Stratton SA, Yang P, Abbas HA, Akdemir ZC, Pant V, Post S, Gagea M, and Lee RG, et al (2015). TRIM24 suppresses development of spontaneous hepatic lipid accumulation and hepatocellular carcinoma in mice. *J Hepatol* **62**(2), 371–379.

[22] Amelio I, Tsvetkov PO, Knight RA, Lisitsa A, Melino G, and Antonov AV (2016). SynTarget: an online tool to test the synergetic effect of genes on survival outcome in cancer. *Cell Death Differ* **23**(5), 912.

[23] Antonov AV (2011). BioProfiling.de: analytical web portal for high-throughput cell biology. *Nucleic Acids Res* **39**(Web Server issue), W323–W327.

[24] Aguirre-Gamboa R, Gomez-Rueda H, Martinez-Ledesma E, Martinez-Torteya A, Chacolla-Huaringa R, Rodriguez-Barrientos A, Tamez-Pena JG, and Trevino V (2013). SurvExpress: an online biomarker validation tool and database for cancer gene expression data using survival analysis. *PLoS One* **8**(9), e74250.

[25] Rhodes DR, Yu J, Shanker K, Deshpande N, Varambally R, Ghosh D, Barrette T, Pandey A, and Chinnaiyan AM (2004). ONCOMINE: a cancer microarray database and integrated data-mining platform. *Neoplasia* **6**(1), 1–6.

[26] Roessler S, Jia HL, Budhu A, Forgues M, Ye QH, Lee JS, Thorgeirsson SS, Sun Z, Tang ZY, and Qin LX, et al (2010). A unique metastasis gene signature enables prediction of tumor relapse in early-stage hepatocellular carcinoma patients. *Cancer Res* **70**(24), 10202–10212.

[27] Wurmbach E, Chen YB, Khitrov G, Zhang W, Roayaie S, Schwartz M, Fiel I, Thung S, Mazzaferro V, and Bruix J, et al (2007). Genome-wide molecular profiles of HCV-induced dysplasia and hepatocellular carcinoma. *Hepatology* **45**(4), 938–947.

[28] Bacher U, Haferlach T, Schoch C, Kern W, and Schnittger S (2006). Implications of NRAS mutations in AML: a study of 2502 patients. *Blood* **107**(10), 3847–3853.

[29] Uhlen M, Zhang C, Lee S, Sjostedt E, Fagerberg L, Bidkhori G, Benfeitas R, Arif M, Liu Z, and Edfors F, et al (2017). A pathology atlas of the human cancer transcriptome. *Science* **357**(6352).

[30] Hashimoto N, Tsunedomi R, Yoshimura K, Watanabe Y, Hazama S, and Oka M (2014). Cancer stem-like sphere cells induced from de-differentiated hepatocellular carcinoma–derived cell lines possess the resistance to anti-cancer drugs. *BMC Cancer* **14**, 722.

[31] Rudalska R, Dauch D, Longerich T, McJunkin K, Wuestefeld T, Kang TW, Hohmeyer A, Pesic M, Leibold J, and von Thun A, et al (2014). In vivo RNAi screening identifies a mechanism of sorafenib resistance in liver cancer. *Nat Med* **20**(10), 1138–1146.

[32] McCormick F (2015). KRAS as a therapeutic target. *Clin Cancer Res* **21**(8), 1797–1801.

[33] Stephen AG, Esposito D, Bagni RK, and McCormick F (2014). Dragging ras back in the ring. *Cancer Cell* **25**(3), 272–281.

[34] Schmick M, Vartak N, Papke B, Kovacevic M, Truxius DC, Rossmannek L, and Bastiaens PI (2014). KRas localizes to the plasma membrane by spatial cycles of solubilization, trapping and vesicular transport. *Cell* **157**(2), 459–471.

[35] Cox AD, Der CJ, and Philips MR (2015). Targeting RAS membrane association: back to the future for anti-RAS drug discovery? *Clin Cancer Res* **21**(8), 1819–1827.

[36] Hou W, Liu J, Chen P, Wang H, Ye BC, and Qiang F (2014). Mutation analysis of key genes in RAS/RAF and PI3K/PTEN pathways in Chinese patients with hepatocellular carcinoma. *Oncol Lett* **8**(3), 1249–1254.

[37] Tolcher AW, Peng W, and Calvo E (2018). Rational approaches for combination therapy strategies targeting the MAP kinase pathway in solid tumors. *Mol Cancer Ther* **17**(1), 3–16.

[38] Sorenson EC, Khanin R, Bamboat ZM, Cavnar MJ, Kim TS, Sadot E, Zeng S, Greer JB, Seifert AM, and Cohen NA, et al (2017). Genome and transcriptome profiling of fibrolamellar hepatocellular carcinoma demonstrates p53 and IGF2BP1 dysregulation. *PLoS One* **12**(5)e0176562.

[39] Ji Y, Wang Z, Li Z, Huang N, Chen H, Li B, and Hui B (2017). Silencing IGF-II impairs C-myc and N-ras expressions of SMMC-7721 cells via suppressing FAK/PI3K/Akt signaling pathway. *Cytokine* **90**, 44–53.

[40] Adhikari H and Counter CM (2018). Interrogating the protein interactomes of RAS isoforms identifies PIP5K1A as a KRAS-specific vulnerability. *Nat Commun* **9**(1), 3646.

[41] D'Alessandro R, Messa C, Refolo MG, and Carr BI (2015). Modulation of sensitivity and resistance to multikinase inhibitors by microenvironmental platelet factors in HCC. *Expert Opin Pharmacother* **16**(18), 2773–2780.

[42] Shi H, Hugo W, Kong X, Hong A, Koya RC, Moriceau G, Chodon T, Guo R, Johnson DB, and Dahlman KB, et al (2014). Acquired resistance and clonal evolution in melanoma during BRAF inhibitor therapy. *Cancer Discov* **4**(1), 80–93.

[43] Hugo W, Shi H, Sun L, Piva M, Song C, Kong X, Moriceau G, Hong A, Dahlman KB, and Johnson DB, et al (2015). Non-genomic and immune evolution of melanoma acquiring MAPKi resistance. *Cell* **162**(6), 1271–1285.

[44] Adams R, Brown E, Brown L, Butler R, Falk S, Fisher D, Kaplan R, Quirke P, Richman S, and Samuel L, et al (2018 Mar). Inhibition of EGFR, HER2, and HER3 signalling in patients with colorectal cancer wild-type for BRAF, PIK3CA, KRAS, and NRAS (FOCUS4-D): a phase 2-3 randomised trial. *Lancet Gastroenterol Hepatol* **3**(3), 162–171

[45] Grabocka E, Pylayeva-Gupta Y, Jones MJ, Lubkov V, Yemanaberhan E, Taylor L, Jeng HH, and Bar-Sagi D (2014). Wild-type H- and N-Ras promote mutant K-Ras-driven tumorigenesis by modulating the DNA damage response. *Cancer Cell* **25**(2), 243–256.